energies

MDPI

Article

Heat Transfer Performance and Influencing Factors of Waste Tires During Pyrolysis in a Horizontal Rotary Furnace

Hongting Ma [1], Yang Bai [1], Shuo Ma [2,*] and Zhipeng Zhou [1]

[1] School of Environmental Science and Engineering, Tianjin University, Tianjin 300350, China; mht116@tju.edu.cn (H.M.); baiyang@hnic.com.cn (Y.B.); 1022214046@tju.edu.cn (Z.Z.)
[2] School of Energy and Safety Engineering, Tianjin Chengjian University, Tianjin 300384, China
* Correspondence: ms0305@tju.edu.cn; Tel.: +86-022-2308-5107

Abstract

Pyrolysis technology currently serves as a significant method for recycling and reducing waste tires. In this paper, in order to improve the heat transfer efficiency during the pyrolysis of waste tires in a horizontal rotary furnace and the yield of pyrolysis oil, the effect laws of tire particle size, rotary furnace rotation speed, enhanced heat transfer materials, and adding spiral fins on heat transfer performance and pyrolysis product distribution were studied, respectively. The innovation lies in two aspects: first, aiming at the problems of slow heat transfer and low pyrolysis efficiency in horizontal rotary furnaces, we identified technical measures through experiments to enhance heat transfer, thereby accelerating pyrolysis and reducing energy consumption; second, with the goal of increasing high-value pyrolysis oil yield, we determined optimal operating parameters to improve economic and sustainability outcomes. The results showed that powdered particles of waste tires were heated more evenly during the pyrolysis process, which increased the overall heat transfer coefficient and the proportion of liquid products. When the rotational speed of the rotary pyrolysis furnace exceeded 2 rpm, there was sufficient contact between the material and the furnace wall, which was beneficial to the improvement of heat transfer performance. Adding heat transfer enhancement materials such as carborundum and white alundum could improve the heat transfer performance between the pyrolysis furnace and the material. Notably, a rotational speed of 3 rpm and carborundum were used as a heat transfer enhancement material with powdered waste tire particles during the pyrolysis process; the overall heat transfer coefficient was the highest, which was 16.89 W/(m^2·K), and the proportion of pyrolysis oil products was 46.1%. When spiral fins were installed, the comprehensive heat transfer coefficient was increased from 12.78 W/(m^2·K) to 16.32 W/(m^2·K). The experimental results show that by increasing the speed of the pyrolysis furnace, adding heat transfer enhancing materials with high thermal conductivity to waste tires, and appropriate particle size, the heat transfer performance and pyrolysis rate can be improved, and energy consumption can be reduced.

Keywords: waste tires; pyrolysis oil; horizontal rotary furnace; heat transfer coefficient

check for updates

Academic Editor: Nicolas Gascoin

Received: 1 July 2025
Revised: 20 July 2025
Accepted: 25 July 2025
Published: 29 July 2025

Citation: Ma, H.; Bai, Y.; Ma, S.; Zhou, Z. Heat Transfer Performance and Influencing Factors of Waste Tires During Pyrolysis in a Horizontal Rotary Furnace. *Energies* **2025**, *18*, 4028. https://doi.org/10.3390/en18154028

Copyright: © 2025 by the authors. Licensee MDPI, Basel, Switzerland. This article is an open access article distributed under the terms and conditions of the Creative Commons Attribution (CC BY) license (https://creativecommons.org/licenses/by/4.0/).

1. Introduction

With the rapid development of domestic transportation and the automotive industry, waste tire generation has surged. As one of the world's largest tire producers (contributing over 30% of global output), China faces pressing challenges in waste tire management—their non-degradability, polluting incineration, and the country's rubber resource shortage

underscore the urgency of high-value utilization. Globally, approximately 1.5 billion waste tires are generated yearly, with China as a top producer. These non-biodegradable tires (due to thermomechanical properties) pose risks: illegal dumping/accumulation may cause uncontrolled combustion, releasing toxins like polycyclic aromatic hydrocarbons. In China, underdeveloped collection systems lead to reliance on landfills/incineration, worsening pollution. Globally, developing nations face backward technologies; developed ones (e.g., the EU, 70–90% recycling) still have residual pollution from incineration [1].

Current waste tire disposal has five limited methods: crumb rubber for roads (toxin leaching), physical-chemical recycling (only for slightly worn tires), incineration/gasification (pollutant emissions), building fillers (structural risks), and landfills (land waste, fire risks). Pyrolysis, by contrast, produces gas (fuel after desulfurization), liquid (C_6–C_{24} hydrocarbons including 25 wt.% limonene), and solid (activatable carbon black) with broad uses. Yet challenges remain: liquid sulfur (1.0–1.75 wt.%), high pretreatment costs, pyrocondensate's high unsaturated hydrocarbons (iodine value 67.8 gI_2/100 g), and sulfur (1.59 wt.%) requiring further processing [2]. Pyrolysis stands out among treatment methods for its small scale, low investment, controllable processes, high-value products (carbon black, combustible gas, pyrolysis oil), and reduced emissions, making it a focus of research [3–7].

Tires consist of natural rubber, synthetic rubber, steel wire, carbon black, and additives. Their pyrolysis involves three key stages: evaporation and decomposition of low-boiling water and additives at 200 °C; onset of rubber pyrolysis with product generation at 300 °C; and near-completion of the reaction at 500 °C [8–10]. During this process, aromatics and saturated hydrocarbons from rubber decomposition undergo cracking (macromolecules breaking into small molecules to form pyrolysis gas, gasoline, diesel, and heavy-oil fractions), while deep cracking leads to polycyclic aromatic condensation in heavy oil, forming coke [3,11].

Waste tire pyrolysis is endothermic, with the pyrolysis degree dependent on external heating and internal heat transfer [12–14]. Influencing factors include reaction conditions (temperature, heating rate), raw material properties (composition, particle size), and reactor structure [13]. Kar et al. found a maximum oil yield of 60.02 wt.% in a fixed bed reactor at a heating rate of 10 °C/min and 425 °C [15]. Galvagno et al. used a pilot-scale rotary kiln (0.4 m diameter, 3 rpm rotation speed) and reported a maximum oil yield of 38.12 wt.% at 550 °C [16].

However, critical gaps exist in current research. Most studies focus on pyrolysis processes and products, with little attention to heat transfer performance and its influencing factors in horizontal rotary furnaces—despite heat transfer directly affecting reaction rate, energy consumption, product distribution, and the technology's practical application.

Horizontal rotary furnaces are widely adopted in industry for their adaptability to raw materials, scalability for continuous operation, and operational flexibility. Yet, their large-volume cylinders cause uneven heat distribution, low heat transfer efficiency, and high energy consumption. Compounding this, pyrolysis in such furnaces involves complex interactions: material mixing, heat/mass transfer between materials and the reactor, and intricate chemical reactions.

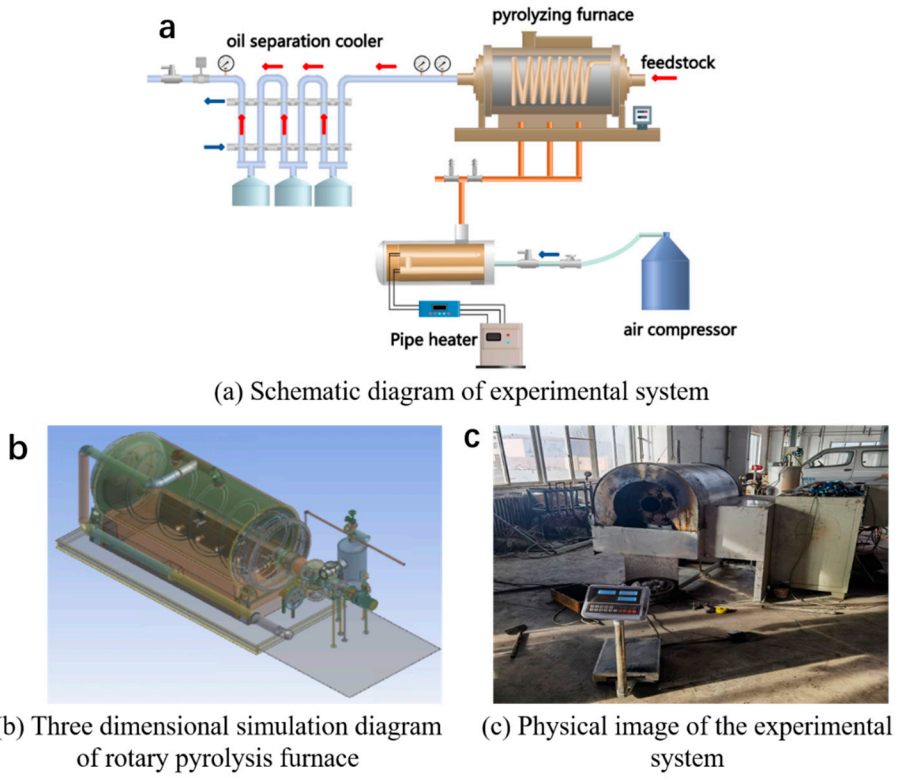
This study addressed these challenges by experimentally analyzing how key factors—waste tire particle size, furnace rotational speed, heat-transfer-enhancing materials, and spiral fins on the pyrolysis chamber outer wall—influence material temperature, heat transfer coefficients, and product distribution. The goal is to identify optimal pyrolysis conditions and heat transfer enhancement measures, thereby improving heat transfer and pyrolysis efficiency and boosting the economic value of products.

The innovation of this article lies in (1) addressing the problems of slow heat transfer rate and low pyrolysis efficiency during the pyrolysis of waste tires in a horizontal rotary furnace, with technical measures being determined through experiments to improve heat transfer performance, thereby accelerating pyrolysis speed and reducing pyrolysis energy consumption; (2) with the goal of increasing the yield of high-value pyrolysis oil, the optimal operating parameters for the pyrolysis process of waste tires were determined through experiments to improve the economy and sustainability of waste tire pyrolysis. Under the conditions of this experiment, when the particle size of waste tires is 1.0–2.3 cm, the rotation speed is 1.5 revolutions per minute, and the enhanced heat transfer material is diamond sand, the yield of pyrolysis oil is the best, and the economy of pyrolysis is the best.

2. Materials and Methods

2.1. Experimental System

To investigate the heat and mass transfer characteristics and influencing factors during the pyrolysis process of waste tires in a horizontal rotary furnace, an experimental system was designed and constructed, as depicted in Figure 1.



(a) Schematic diagram of experimental system

(b) Three dimensional simulation diagram of rotary pyrolysis furnace

(c) Physical image of the experimental system

Figure 1. Diagram of horizontal pyrolysis experimental device for waste tires.

The length of the pyrolysis furnace is 1.1 m, the inner diameter of the cylinder is 0.414 m, the outer diameter is 0.426 m, and the outer surface area is 1.47 m^2.

The system predominantly consisted of a horizontal rotary pyrolysis furnace, pipeline heater, air compressor, oil separation cooler, temperature measurement system, and pyrolysis product collection system. For this experiment, specialized pipeline heating furnaces and air compressors were employed to provide high-temperature gas, achieving a peak temperature of 800 °C. The oil-separating cooler was constructed as a double-pipe heat exchanger, with cooling water circulating through the outer pipe and the volatile gas generated in the pyrolysis furnace passing through the inner pipe. Upon cooling, the

gas and oil were efficiently separated. The temperature monitoring system incorporated wireless temperature sensors, enabling real-time tracking of temperature variation within the materials in the furnace and the high-temperature air.

In this study, three horizontal heat-resistant stainless steel sleeves were installed in the pyrolysis chamber, with one horizontal heat-resistant sleeve installed near the bottom of the pyrolysis chamber to come into contact with the waste tire particle layer throughout the pyrolysis process. Five K-type thermocouples were arranged on each sleeve to measure the temperature distribution of different sizes of waste tire particle layers, as shown in Figure 2. All numbers in the picture are in millimeters.

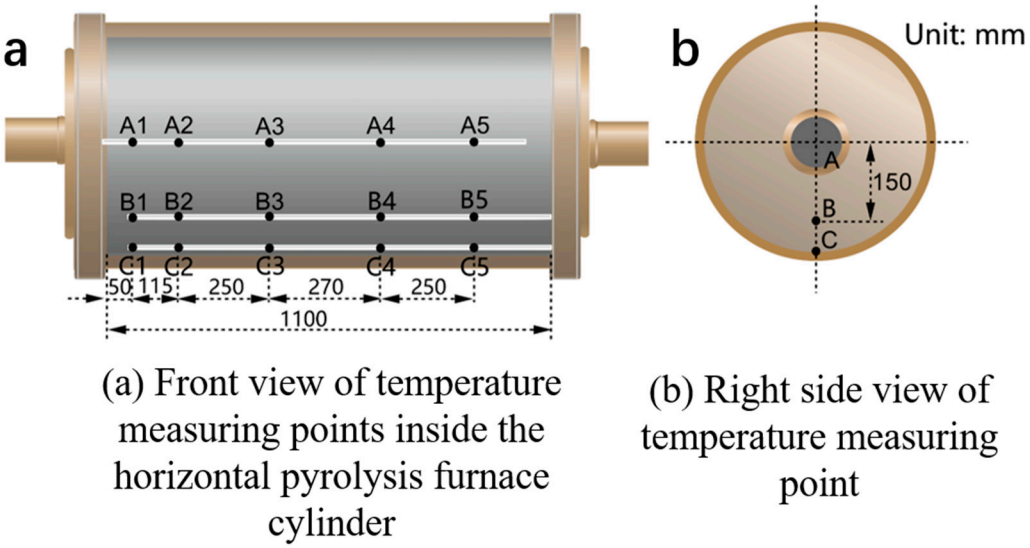


Figure 2. Schematic diagram of temperature measuring point in the inner cylinder of horizontal pyrolysis furnace.

2.2. Experimental Materials and Conditions

The waste tires used in this experiment are car tires, which are mainly used for transportation vehicles such as passenger cars and commercial vehicles. They are the main type of waste tires. The experiments were carried out on four kinds of particle sizes: powder, fine, medium, and coarse. The corresponding density and particle size were presented in Table 1 below.

Table 1. Density and particle size of different particle types.

Particle Type	Density (kg/m^3)	Size (cm)
Powder	414	<0.1
Fine	470	0.3~2.1
Medium	446	1.0~2.3
Coarse	421	2.0~3.0

The experimental conditions were as follows: the hot gas flow rate was 24 m^3/h, the pyrolysis final temperature was 470 °C, the pyrolysis furnace speed n = 1~3 rpm, the experimental material mass was 10 kg, and the addition amount of heat transfer enhancement material was 5 kg.

Due to the fact that the waste tires had been crushed into small particles with a diameter of less than 3 mm before the experiment, and the metal cords were sorted out, the pyrolysis products did not contain metal cords.

2.3. Method for Calculating the Heat Transfer Coefficient of a Rotary Furnace

The heat transfer process during the pyrolysis of waste tires in a rotary pyrolysis furnace consists of three parts: the convection heat transfer between the high-temperature gas and the outer wall surface of the inner cylinder of rotary pyrolysis furnace, the heat conduction of the cylinder body in rotary pyrolysis furnace, and the heat transfer between the inner wall surface of the inner cylinder of rotary pyrolysis furnace and waste tire particles [16–18].

(1) The convective heat transfer coefficient between the high-temperature gas and the outer wall of the inner cylinder in a rotary pyrolysis furnace.

The convective heat transfer coefficient $\alpha_{aw,\lambda}$ between high-temperature gas and the outer wall of the rotary pyrolysis furnace can be calculated by the energy balance calculation formula as follows:

$$\alpha_{aw,\lambda} \cdot A_{aw} \cdot \Delta T = Q_1 + Q_2 + Q_3 + Q_4, \quad (1)$$

$$Q_1 = M_r \cdot C_{p,r} \cdot \frac{dT_{r,m}}{dt}, \quad (2)$$

$$Q_2 = M_s \cdot C_{p,s} \cdot \frac{dT_{s,m}}{dt}, \quad (3)$$

$$Q_3 = M_o \cdot C_{p,o} \cdot \frac{dT_{o,m}}{dt}, \quad (4)$$

where Q_1 is the heat absorbed by the inner cylinder, W. Q_2 is the heat taken away by the material in the inner cylinder, W. Q_3 is the heat taken away by oil and gas during pyrolysis, W. Q_4 is the various heat losses through the brick masonry of the base of the outer cylinder, the insulation layer of the outer cylinder, the two end faces of the inner cylinder, the rolling ring, the gear ring, and the furnace door. It is initially set as 20% of the total energy from the high-temperature gas, based on experience, W. A_{aw} is the outer wall area of the inner cylinder of the rotary pyrolysis furnace, m^2. t is the pyrolysis time, s. M_r is the inner tube mass of the rotary pyrolysis furnace, kg. $T_{r,m}$ is the average temperature of the inner cylinder of the rotary pyrolysis furnace, °C. $C_{p,r}$ is the heat capacity of the inner cylinder of the rotary pyrolysis furnace at constant pressure, J/kg·K. M_s is the mass of waste tire involved in the pyrolysis reaction, kg. $T_{s,m}$ is the average temperature of the waste tire involved in the pyrolysis reaction, °C. $C_{p,s}$ is the heat capacity of waste tire material at constant pressure, J/kg·K. M_o is the mass of oil and gas produced by pyrolysis, kg. $T_{o,m}$ is the average temperature of oil and gas produced by pyrolysis, °C. $C_{p,o}$ is the heat capacity of oil and gas produced by pyrolysis at constant pressure, J/kg·K.

(2) Thermal conductivity of the inner cylinder

The inner cylinder is made of 304 steel, and the thermal conductivity is 16.3 W/(m·K) at 100 °C and 21.5 W/(m·K) at 500 °C. The thermal conductivity kt is calculated by interpolation according to the arithmetic average of the temperature of the inner wall and the outer wall of the inner cylinder.

(3) The apparent heat transfer coefficient between the inner surface of the inner cylinder of the pyrolysis furnace and the material

The apparent heat transfer coefficient between the inner wall and the material in the inner cylinder of the rotary pyrolysis furnace is a crucial parameter for describing the heat transfer efficiency, which is defined as the ratio of the heat transferred through the inner wall per unit area in a unit time to the temperature difference between the inner wall and the material. In order to determine the apparent heat transfer coefficient, it is considered that the pyrolysis chamber is energy balanced, assuming that the total energy from the wall is transferred to the material bed and absorbed by the material. Given that

the thermal resistance of waste tire substantially surpasses that of the thermal resistance of the contact gap between the material bed and the wall, the impact of the contact gap between the material bed and the wall on the apparent heat transfer coefficient is ignored. The apparent heat transfer coefficient between the wall and the material is calculated by the energy balance formula as follows [19]:

$$\alpha_{ws,\lambda} \cdot A_{w,s} \cdot (T_w - T_{s,m}) = M_s \cdot C_{p,s} \cdot \frac{dT_{s,m}}{dt}, \quad (5)$$

where A_{ws} is the contact area between cylinder wall and material bed in the rotary pyrolysis furnace, which is related to filling degree, m^2. T_w is the temperature of cylinder wall in the rotary pyrolysis furnace, °C.

The variation of apparent heat transfer coefficient between the wall and the material can be obtained according to the temperature distribution data measured in the experiment over time.

(4) The comprehensive heat transfer coefficient of rotary pyrolysis furnace

After calculating the convection heat transfer coefficient between high-temperature gas and the outer wall of the inner cylinder of the rotary pyrolysis furnace, the thermal conductivity coefficient of the cylinder in the rotary pyrolysis furnace, and the apparent heat transfer coefficient between the inner wall of the inner cylinder of the rotary pyrolysis furnace and waste tire particles, the comprehensive heat transfer coefficient K of the rotary pyrolysis furnace was calculated according to the following formula:

$$K = 1 / \left(\frac{1}{\alpha_{aw,\lambda}} + \frac{k_t A_{aw}}{\delta} + \frac{1}{\alpha_{ws,\lambda}} \right) \quad (6)$$

where δ is the thickness of the inner cylinder of the rotary pyrolysis furnace, m.

3. Results and Discussion

3.1. Effect of Waste Tire Particle Size on Heat Transfer Performance and the Distribution of Pyrolysis Products

There was a certain impact of particle size on the material temperature distribution, heat transfer performance, and pyrolysis reaction rate during the pyrolysis process. Therefore, pyrolysis experiments were carried out using waste tires with particle sizes of powdered, fine, medium, and coarse, respectively. The temperature changes of the materials and the composition of the pyrolysis products during the pyrolysis process were measured, and the influence of tire particle size on heat transfer performance and product distribution was analyzed.

Figure 3 shows the variation in temperature with time during the pyrolysis process of waste tires with four particle sizes of powdered, fine, medium, and coarse.

The experimental results showed that the temperature variation trends for waste tires of different particle sizes during the pyrolysis process were basically the same. The maximum temperature disparity between material layers of different particle sizes was noted as 12.1 °C.

In the initial stage (0~2 h), there was little effect of particle size on the temperature change of the materials, and the heating rate was about 3.01 °C/min. It indicated that the heating process of the materials at this stage was mainly affected by the overall heating conditions, rather than the particle size.

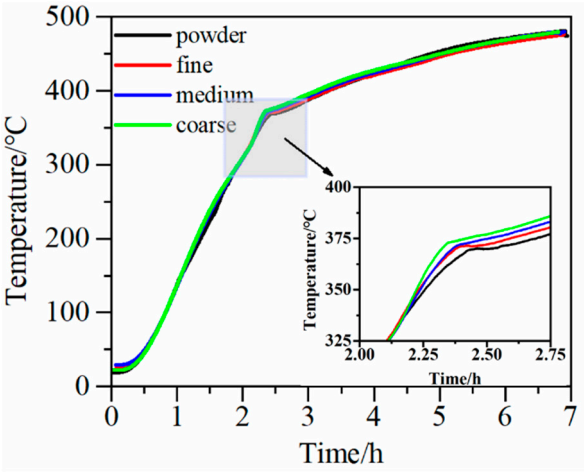


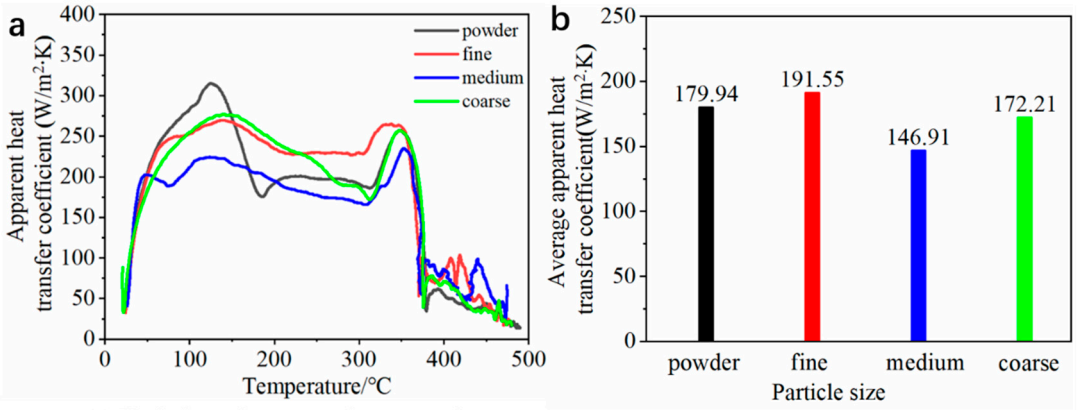
Figure 3. The temperature of waste tires with different particle sizes varies with the pyrolysis time.

Upon reaching an approximate temperature of 340 °C in the material layer, the waste tires proceed into the pyrolysis stage, and the change rate of temperature begins to exhibit variations among different particle sizes. Especially in the period from 2.25 to 2.75 h, the heating rate decreased with decreasing particle size. It was attributed to the fact that pyrolysis is an endothermic reaction. Smaller particles possess a larger specific surface area, which enhances the contact with the inner surface of the pyrolysis chamber. It facilitated the heat transfer effect, enabling the particles to absorb more heat within the same time, and the pyrolysis reaction rate was faster. However, the majority of the absorbed heat was utilized for the pyrolysis reaction, which resulted in a relatively low heating rate. In contrast, larger particles resulted in nonuniform heat transfer; their pyrolysis reaction rate was slower, less heat was absorbed and mainly used for temperature rise, and their temperature rising rate was obviously higher than that of small particle tires. When the temperatures of the material layers of the four types of particles (powdered, fine, medium, and coarse) rose to 373.1 °C, 371.5 °C, 370.6 °C, and 369.4 °C, the heating rate decreased significantly. It indicated that the materials began to rapidly pyrolyze, accompanied by significant heat adsorption, resulting in a marked decrease in the heating rate.

As the pyrolysis progresses, the temperature variations of the material layers with different sizes gradually became uniform, and the heating rate decreased to approximately 0.56 °C/min. When the temperature of the material layer reached 400 °C, the pyrolysis reaction basically came to an end. The remaining solid residue mainly consisted of inorganic substances such as carbon black and fibers, and their particle size effect became negligible. Notably, the temperatures of tires with different particle sizes were very close, with a maximum temperature difference of only 3.9 °C.

To intuitively illustrate the heat transfer rate during the pyrolysis process, the measured temperature distribution data were used to calculate the apparent heat transfer coefficients of waste tire particles with different particle sizes. The results were shown in Figure 4.

As can be seen from Figure 4a, the apparent heat transfer coefficients corresponding to different particle sizes exhibited a bimodal distribution as temperature altered during the pyrolysis process. In the initial stage, the first peak appeared at approximately 130 °C, followed by a second peak around 370 °C. When the temperature was higher than 400 °C, the apparent heat transfer coefficient dropped rapidly to a relatively lower value and subsequently decreased slowly.



(a) Variation of apparent heat transfer coefficient with temperature

(b) Average apparent heat transfer coefficient

Figure 4. Heat transfer performance between the inner wall of the pyrolysis furnace and the material during the pyrolysis of waste tires with different particle sizes.

The main reasons for the above-mentioned phenomenon can be attributed to the following. In the initial stage of pyrolysis, the waste tire particles retained their original appearance, and they were not deformed by heat. The gaps between the particles resulted in poor thermal conductivity, making it difficult to transfer heat to the interior of the material. Therefore, the external temperature of materials rose quickly, leading to a large temperature gradient between the interior and exterior. Moreover, given that evaporation is an endothermic process, the evaporation of water and low-boiling-point additives in materials requires absorbing substantial heat. Consequently, the heating rate was slow, leading to an increase in the temperature gradient of the tire. In addition, with the increase in temperature, more water vapor was generated. The disturbance of water vapor would strengthen the heat transfer effect, so the apparent heat transfer coefficient increased rapidly, reaching an extremum at about 130 °C.

As the temperature continued to rise, the waste tires appeared to be partially softened and agglomerated. The closer contact between the particles resulted in a more uniform heating, leading to a reduced temperature gradient. Therefore, the apparent heat transfer coefficient decreased to some extent.

When the temperature of the materials rose to around 340 °C, waste tires began to undergo pyrolysis reaction. However, the pyrolysis reaction process requires absorbing a large amount of heat, which increases the temperature gradient inside the materials and promotes the transfer of heat from the wall surface to the interior of the materials. Meanwhile, the gas and liquid products generated during the pyrolysis increase the specific surface area and fluidity of the materials, further improving the heat transfer performance. In addition, with the increase in temperature, the radiation heat transfer between the surface of the pyrolysis chamber and the materials was enhanced, resulting in an increase in the apparent heat transfer coefficient. As the pyrolysis reaction proceeded, the temperature in the material bed gradually reached a state of equilibrium, and the temperature gradient stabilized with minimal variation.

When the temperature reached about 400 °C, the pyrolysis process essentially ended. The majority of the organic substances in the materials had been decomposed, and the remaining solid residue exhibited poor thermal conductivity, so the apparent heat transfer coefficient decreased.

Upon analyzing the data from the entire pyrolysis process, the average apparent heat transfer coefficients corresponding to different particle sizes were obtained, as illustrated in Figure 4b. It can be seen that the average apparent heat transfer coefficient of fine

particle waste tires was the largest with 191.55 W/(m^2·K), and the average apparent heat transfer coefficient of powder, medium, and coarse particles was 179.94 W/(m^2·K), 146.91 W/(m^2·K), and 172.21 W/(m^2·K), respectively.

The main reason for the highest average apparent heat transfer coefficient corresponding to fine particle waste tires is that the average apparent heat transfer coefficient is related to the contact area between the waste tire particles and the surface inside the pyrolysis chamber, as well as the contact thermal resistance between the particles. When the quality of experimental materials is the same, the smaller the particle size, the higher the packing density of the material layer, and the lower the contact thermal resistance between particles, which has a positive effect on heat transfer. However, the decrease in particle size reduces the contact area between the material and the surface inside the pyrolysis chamber, which has an adverse effect on heat transfer. Under the combined action of these two factors, the comprehensive heat transfer effect of fine particulate materials reaches its optimum, and the average apparent heat transfer coefficient reaches its maximum value.

During the pyrolysis process, the comprehensive heat transfer coefficient between the inner wall of the pyrolysis furnace and the material when using waste tires with different particle sizes is shown in Figure 5.

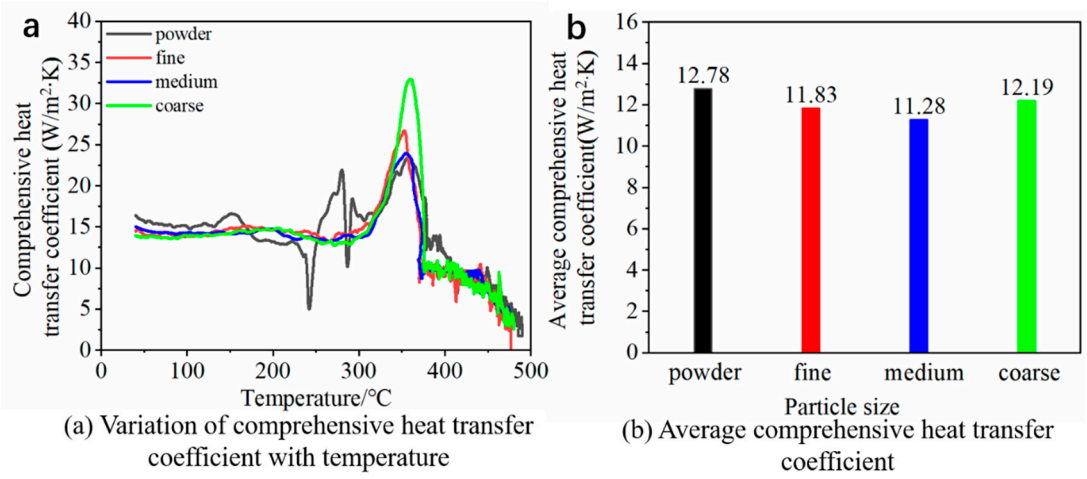


Figure 5. Comprehensive heat transfer performance during pyrolysis of waste tires with different particle sizes.

The heat transfer coefficient increased slightly in the initial stage of pyrolysis. However, upon transitioning into the pyrolysis process, the heat transfer coefficient increased rapidly and reached its maximum value near 380 °C, which corresponded to the temperature at which the maximum thermogravimetric rate of waste tire occurred. Subsequently, a significant decrease in the yield of pyrolysis gas was observed due to the deceleration of the pyrolysis rate, and the comprehensive heat transfer coefficient dropped rapidly as well. When the pyrolysis temperature exceeded 400 °C, the pyrolysis process basically completed, with the comprehensive heat transfer coefficient maintaining a low level and gradually decreasing.

As can be seen from Figure 5b, the average comprehensive heat transfer coefficients for the four particle sizes were 12.78 W/(m^2·K), 11.83 W/(m^2·K), 11.28 W/(m^2·K), and 12.19 W/(m^2·K), respectively. Contrary to the average apparent heat transfer coefficient, the average comprehensive heat transfer coefficient of the pyrolysis furnace is the highest when the waste tire particles are powder. This is mainly because the small particles with lower mass are more readily carried by the flow in the high-temperature gas. Thus, the degree of turbulence of the gas was increased, and the mixing and momentum exchange inside the gas were enhanced. The enhanced turbulence effect can effectively break the thermal

boundary layer, thereby accelerating the rate of heat transfer. As a result, the convective heat transfer coefficient was increased, thus increasing the average comprehensive heat transfer coefficient.

During the pyrolysis of waste tire particles in a horizontal rotary furnace, liquid, gaseous, and solid products are generated, and the pyrolysis products of tires with different particle sizes were collected and analyzed, as shown in Figure 6.

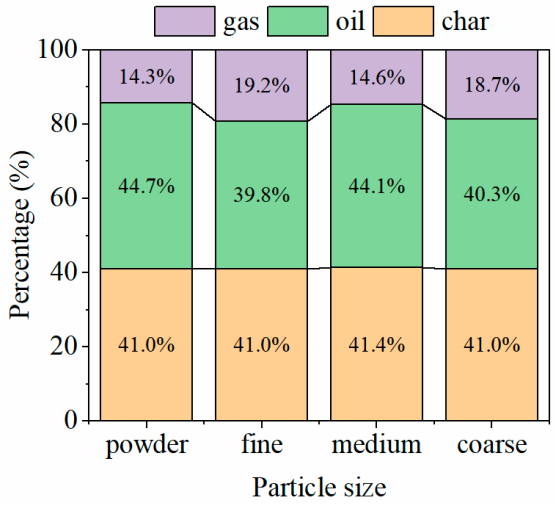


Figure 6. Effect of particle size of waste tire on distribution of pyrolysis products.

The waste tires used in the experiment were relatively clean, and the content of metals, quartz sand, or white corundum in the carbon black was very low, so other impurities were not considered when weighing the pyrolysis solid product.

As illustrated in Figure 6, the mass of solid products remaining after the pyrolysis of tires with different particle sizes was essentially the same, approximately 41%. However, the proportions of liquid and gaseous products were different. The yield of liquid products from powdered and medium tire particles was relatively high, reaching 44.7% and 44.1%, respectively. It might be because smaller particles possess a larger specific surface area, enabling them to absorb heat more uniformly. Consequently, the pyrolysis reaction was facilitated to proceed more thoroughly, generating more liquid products. In particular, powdered particles experienced a more uniform heating process, and their pyrolysis process reached thermal equilibrium rapidly. It prevented secondary cracking of liquid products caused by local overheating, consequently resulting in a higher yield of liquid products [20].

For fine and coarse particles of waste tires, the yields of liquid products were low (39.8% and 40.3%), and gaseous products were relatively high (19.2% and 18.8%, respectively), but the reasons were different. Fine particles, with a relatively broad size range, nonuniform particle sizes, and high bulk density, lead to significant local overheating. As a result, liquid products were further decomposed into gaseous products under high temperature conditions. For coarse particles, the low bulk density with high porosity resulted in poor heat transfer performance, which led to a significant temperature gradient. Owing to the low thermal conduction efficiency, the pyrolysis reaction was incomplete; some of the raw materials failed to be fully converted into liquid products and instead directly volatilized into gaseous substances, leading to an increase in the proportion of gaseous products [21,22].

Under the same final pyrolysis temperature, the yield of pyrolysis oil is mainly related to the heating rate of waste tires. The key factors affecting the heating rate include particle size, contact heat transfer between particles, and heat transfer process between particles and the surface inside the pyrolysis chamber. According to the experimental results of this

article, it is possible that the heating rates of powdered particles and medium particles in the pyrolysis chamber are relatively high and close, so the pyrolysis oil yield is also relatively close.

3.2. Effect of Rotational Speed on Heat Transfer Performance and the Distribution of Pyrolysis Products

The rotational speed of the rotary pyrolysis furnace can affect the pyrolysis efficiency of waste tires and thus influence the degree of pyrolysis. Therefore, we explored the variation of the average temperature of the materials in the pyrolysis chamber over time at different rotational speeds, as shown in Figure 7.

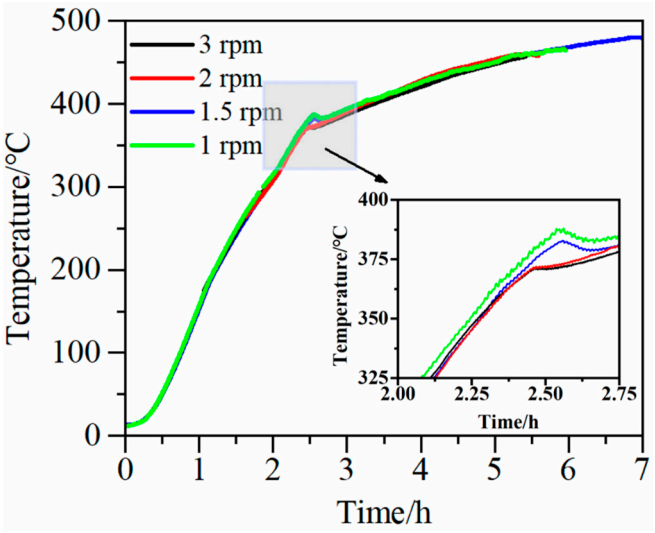
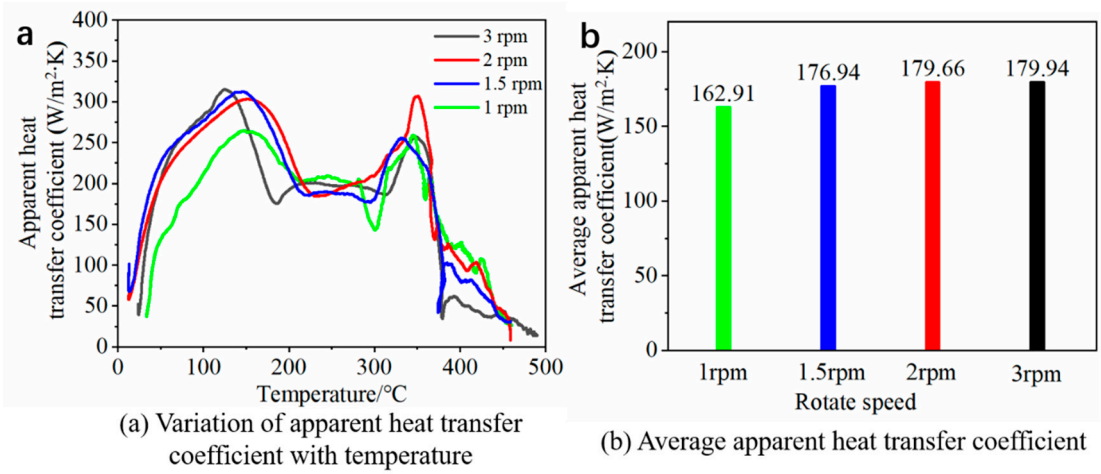


Figure 7. The temperature of waste tires with different pyrolysis furnace speeds.

From Figure 7, the temperature variation trends of waste tires in the pyrolysis chamber were basically consistent at different speeds. Within 2.25 h after the beginning of heating, the rotational speed had almost no effect on the temperature of the materials. After that, the influence of the rotational speed gradually appeared. When the temperature of the material layer rose to around 340 °C, the waste tires began to pyrolyze, which was an endothermic reaction. The heating rate decreased, and the influence of the rotational speed on the temperature of the materials appeared different. Within the 2.25 to 2.75 h, the temperature of the materials corresponding to a higher rotational speed was slightly lower than that of a lower rotational speed, with a maximum temperature difference of 16.2 °C. It was because as the rotational speed increased, the contact between the materials and the pyrolysis chamber wall became more sufficient. More heat was transferred from the outside of the pyrolysis chamber, and the temperature distribution within the materials was more uniform. The materials absorbed more heat during the pyrolysis reaction, resulting in a slower increase in the materials' temperature.

When the temperature of the material layer reached 400 °C, the pyrolysis reaction was almost finished. The fewer remaining components, the less the influence of the rotational speed on the temperature of the materials, which gradually becomes consistent.

To illustrate the influence of the rotational speed of the pyrolysis furnace on heat transfer performance, the apparent heat transfer coefficients between the inner wall of the inner cylinder of the rotary pyrolysis furnace and the material at the rotational speeds of 1 rpm, 1.5 rpm, 2 rpm, and 3 rpm were calculated, respectively, as shown in Figure 8.



(a) Variation of apparent heat transfer coefficient with temperature

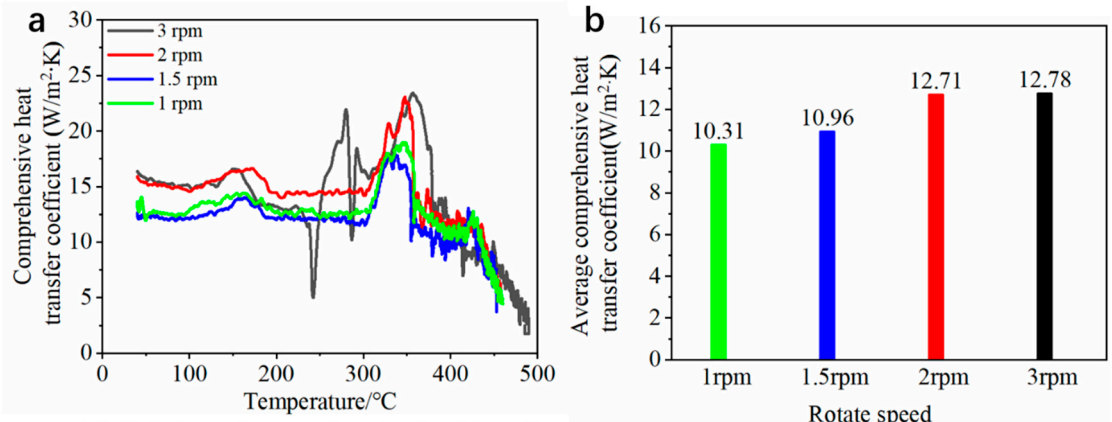
(b) Average apparent heat transfer coefficient

Figure 8. Heat transfer performance between the inner wall of the inner cylinder and the material in the pyrolysis furnace at different speeds.

As can be seen from Figure 8a, the apparent heat transfer coefficient between the pyrolysis furnace and the materials at different stages presented different trends during the pyrolysis process. At the beginning, it was increased with the rise of temperature, reached a maximum value at 135 °C, and then decreased, entering a plateau period. When the temperature reached 340 °C, there was a notable increase in the apparent heat transfer coefficient with the increase in temperature. It subsequently reached a maximum value at 370 °C, before undergoing a decrease.

As shown in Figure 8b, the apparent heat transfer coefficients at the four rotational speeds of 1 rpm, 1.5 rpm, 2 rpm, and 3 rpm were 162.91 W/(m^2·K), 176.94 W/(m^2·K), 179.66 W/(m^2·K), and 179.94 W/(m^2·K), respectively. As the rotational speed increased, the heat transfer coefficient also increased. When the rotational speed increased to 2 rpm, the heat transfer coefficient almost no longer changed. The increased rotational speed ensured a more sufficient contact between the materials and the chamber wall, enabling the apparent heat transfer coefficient between the inner wall of the pyrolysis furnace and the materials to reach a relatively higher value [23,24].

The instantaneous comprehensive heat transfer coefficient of the horizontal rotary pyrolysis furnace and temperature, as well as the average comprehensive heat transfer coefficient, when the rotational speeds of the horizontal rotary pyrolysis furnace were 1 rpm, 1.5 rpm, 2 rpm, and 3 rpm, respectively, are shown in Figure 9.



(a) Variation of comprehensive heat transfer coefficient with temperature

(b) Average comprehensive heat transfer coefficient

Figure 9. Comprehensive heat transfer performance of pyrolysis furnaces at different rotational speeds.

As shown in Figure 9a, the variation trends of the instantaneous comprehensive heat transfer coefficient at different rotational speeds with temperature during the pyrolysis process exhibited almost unanimously, all presenting a bimodal pattern. The first peak appeared at about 180 °C, followed by a second peak at around 370 °C. Thereafter, a dramatic decrease was observed after 400 °C, eventually leading to a slow change. The main factor contributing to this transformation was the evaporation of water in the initial and the accelerated pyrolysis occurring in the subsequent stage.

For Figure 9b, the average comprehensive heat transfer coefficients of the rotary pyrolysis furnace with the rotational speeds of 1 rpm, 1.5 rpm, 2 rpm, and 3 rpm were 10.31 W/(m^2·K), 10.96 W/(m^2·K), 12.71 W/(m^2·K), and 12.78 W/(m^2·K), respectively. It indicated that the average comprehensive heat transfer coefficient increased as the rotational speed increased accordingly. The acceleration of the rotational speed resulted in an increase in both the frequency and intensity of the materials being agitated in the pyrolysis furnace. The contact between the materials became more sufficient, and there were more heat transfer paths, enabling heat to be transferred more easily within the materials. A higher rotational speed made the gas boundary layer on the surface of the materials thinner, reducing the resistance to heat transfer. Thus, the heat exchange between the high-temperature gas and the materials became easier, and the heat transfer performance was enhanced.

In order to analyze the influence of the rotational speed of the horizontal pyrolysis furnace on the distribution of pyrolysis products, the mass of solid, liquid, and gaseous products during the pyrolysis of waste tires at different rotational speeds was collected and analyzed. The results were shown in Figure 10.

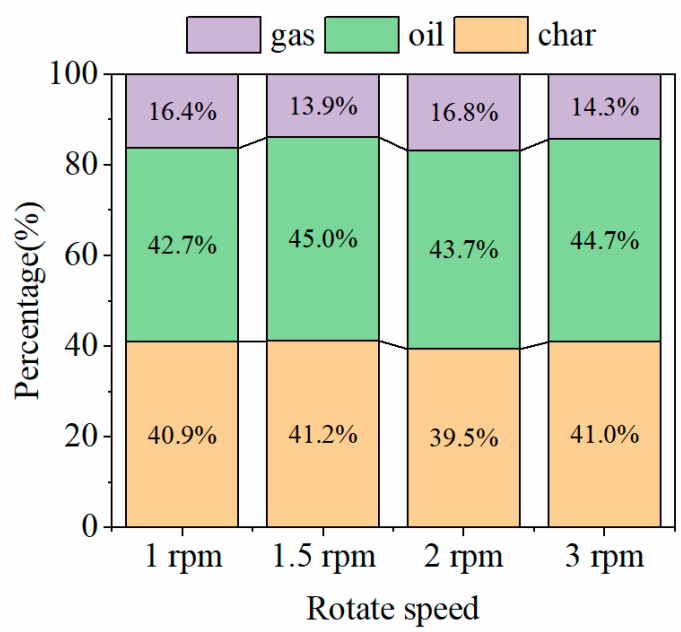


Figure 10. Effect of pyrolysis furnace rotation speed on the distribution of pyrolysis products.

As depicted in Figure 10, the mass of solid products remained relatively consistent at different rotational speeds, with the maximum relative deviation being only 4.1%. When the rotational speed exceeded 1.5 rpm, there was a slight increase in liquid products and a corresponding decrease in gaseous products. This phenomenon can be attributed to the higher rotational speeds, which reduced the residence time of pyrolysis oil in the high-temperature environment, thereby inhibiting further pyrolysis into gaseous products.

3.3. Effect of Heat Transfer Enhancement Materials on Heat Transfer Performance and the Distribution of Pyrolysis Products

To further enhance the heat transfer efficiency during the pyrolysis process, three materials, including carborundum, quartz sand, or white alundum, were chosen as enhanced heat transfer materials incorporated into waste tires. The variation of the material temperature over time is shown in Figure 11.

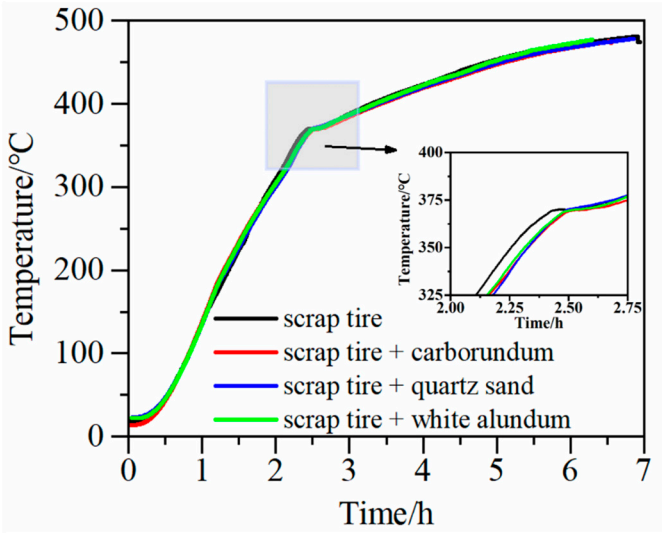


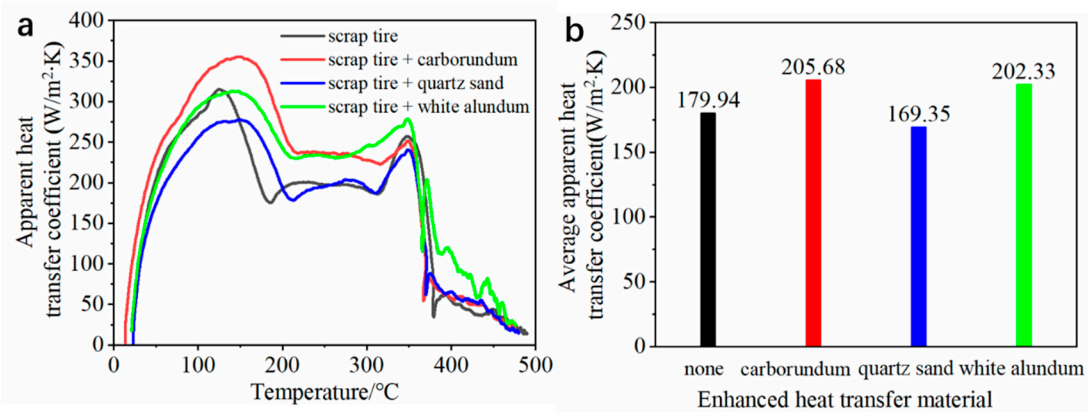
Figure 11. The temperature of waste tires over time when adding different enhanced heat transfer materials.

As illustrated in Figure 11, the temperature of waste tires mixed with different enhanced heat transfer materials showed a trend of rapid increase at the beginning, followed by a slower increase. In the first 2 h of the pyrolysis process, prior to the commencement of the pyrolysis reaction, the heating rate of waste tires alone and those with different materials added was around 3.0 °C/min. When the pyrolysis reaction began, the heating rate for mixtures containing heat transfer enhancement materials and waste tires decreased slightly. It was attributed to the enhanced heat transfer materials that improve the heat transfer efficiency, which was beneficial for waste tires to absorb heat for the pyrolysis reaction. When the temperature reached approximately 370 °C, the pyrolysis reaction became vigorous and required substantial heat adsorption, resulting in a marked decrease in the heating rate.

According to the measured material temperature, the apparent heat transfer coefficient between the material and the inner surface of the pyrolysis furnace after adding different enhanced heat transfer materials can be obtained through calculation, as depicted in Figure 12.

As can be seen from Figure 12a, it was evident that the variation trends of the apparent heat transfer coefficients of waste tires alone and mixtures with enhanced heat transfer materials were fundamentally identical, both showing a bimodal pattern. During the pyrolysis process, the first peak appeared at around 130 °C in the initial stage, and the second peak occurred at about 370 °C.

By analyzing the instantaneous apparent heat transfer coefficient in Figure 12a, the average apparent heat transfer coefficients for the pyrolysis of waste tire alone and mixtures with carborundum, quartz sand, and white alundum were determined, respectively. As shown in Figure 12b, the values were 179.94 W/(m^2·K), 205.68 W/(m^2·K), 169.35 W/(m^2·K), and 202.33 W/(m^2·K), respectively.



(a) Variation of apparent heat transfer coefficient with temperature

(b) Average apparent heat transfer coefficient

Figure 12. Heat transfer performance between the inner wall of the pyrolysis furnace and materials with different heat transfer enhancement materials.

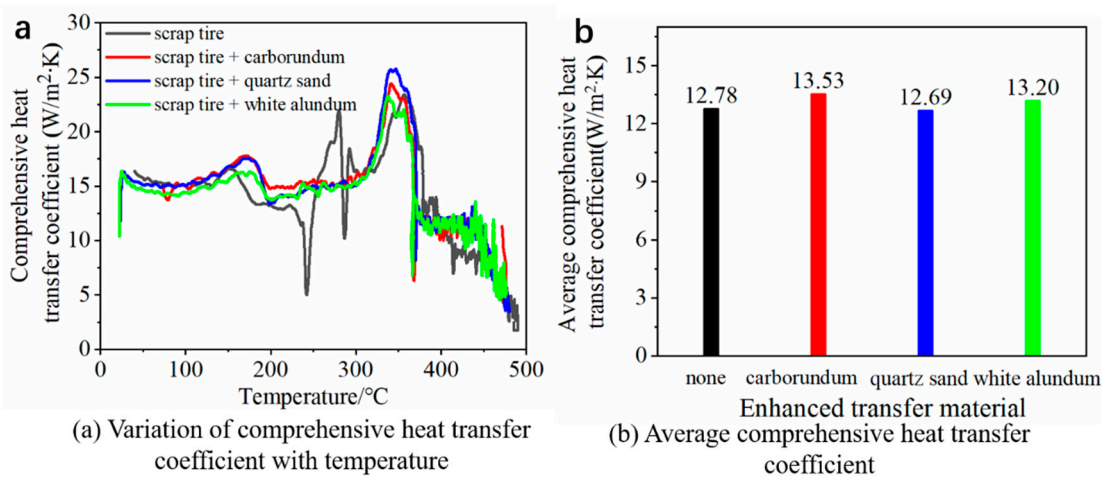
The heat transfer performance can be significantly enhanced after incorporating carborundum and white alundum, while the effect of quartz sand was not obvious. The main reasons were as follows. On the one hand, the thermal conductivity of carborundum is 135.6 W/(m·K), and that of white alundum is 20~30 W/(m·K), which are both significantly higher than that of quartz sand, which is 1~10 W/(m·K). Materials with high thermal conductivity establish more efficient heat conduction paths within the material, enabling faster heat transfer and improving heat transfer efficiency during the thermal exchange process. On the other hand, the coefficient of thermal expansion also significantly influenced the heat transfer efficiency. The coefficients of thermal expansion of carborundum, white alundum, and quartz sand are 4~5 $\times$ 10^{-6}/°C, 8~9 $\times$ 10^{-6}/°C, and 5.5 $\times$ 10^{-7}/°C, respectively. Appropriate expansion enhanced the contact area and tightness between the enhanced heat transfer materials and the surrounding medium (such as pyrolysis gas or heated materials), facilitating the heat transfer [25–32].

Additionally, the heat transfer performance was also influenced by the density of enhanced heat transfer materials. During the process of heat conduction, heat was transferred through the vibration of atoms and molecules or the movement of free electrons. The densities of carborundum, white alundum, and quartz sand are 3.06~3.20 g/cm^3, 3.95~4.00 g/cm^3, and 2.65 g/cm^3, respectively. Materials with higher density typically feature more closely packed atoms or molecules, forming a tightly connected "heat transfer chain" that enables more efficient heat transfer within the material.

The comprehensive heat transfer coefficients after adding three enhanced heat transfer materials of carborundum, quartz sand, and white alundum are shown in Figure 13.

It can be observed that the comprehensive heat transfer coefficients for the pyrolysis of waste tires alone and with the addition of carborundum, quartz sand, and white alundum were 12.78 W/(m^2·K), 13.53 W/(m^2·K), 12.69 W/(m^2·K), and 13.20 W/(m^2·K), respectively. Among them, carborundum exhibited the best heat transfer enhancement effect, followed by white alundum, with quartz sand being the least effective.

Compared with the particle size of waste tires and the rotation speed of the pyrolysis furnace, the enhanced heat transfer materials with the most significant impact on heat transfer performance could effectively improve pyrolysis efficiency and reduce energy consumption.



(a) Variation of comprehensive heat transfer coefficient with temperature

(b) Average comprehensive heat transfer coefficient

Figure 13. Comprehensive heat transfer performance after adding different enhanced heat transfer materials.

The mass of solid, liquid, and gaseous products of waste tire pyrolysis after mixing with different enhanced heat transfer materials was collected and analyzed. The distribution of pyrolysis products is shown in Figure 14.

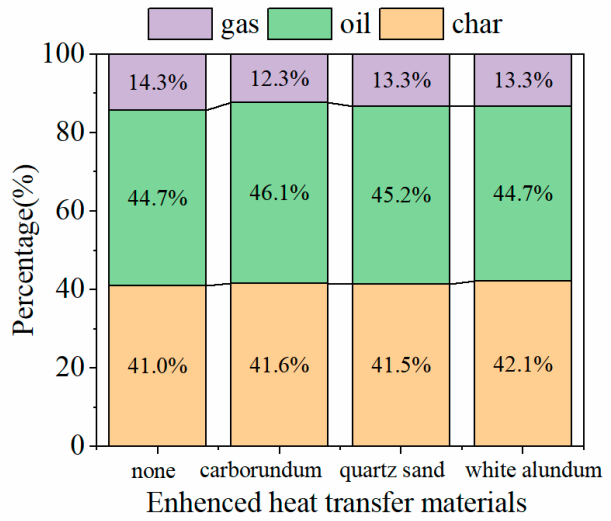


Figure 14. Effect of enhanced heat transfer materials on the distribution of pyrolysis products.

The results indicated that adding enhanced heat transfer materials had minimal impact on the solid products in the pyrolysis products, maintaining it at approximately 41%. After adding carborundum and quartz sand, the proportion of liquid products increased from 44.7% to 46.1% and 45.2%, respectively, while the proportion of gaseous products decreased from 14.3% to 12.3% and 13.3%. In contrast, adding white alundum had little effect on the liquid product fraction but slightly reduced the gaseous product fraction from 14.3% to 13.3%.

3.4. Effect of Installing Spiral Fins on Heat Transfer Performance

Owing to the superior heat transfer performance and space-saving characteristics, spiral finned tubes were prevalently employed in heat exchange equipment. To enhance heat transfer efficiency, spiral fins were installed in this study, and the variation trends of material temperature with time were monitored, as shown in Figure 15.

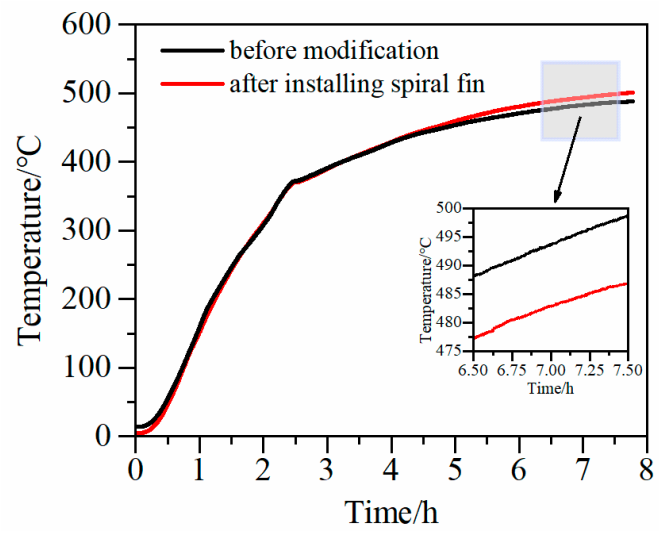
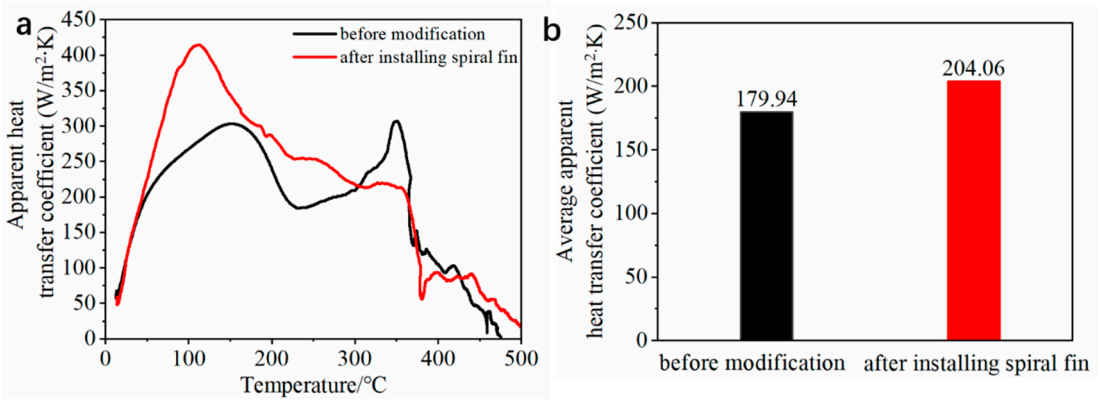


Figure 15. The temperature of waste tires over time when installing spiral fins.

As can be seen from Figure 15, the general trend of material temperature variation during the pyrolysis process of waste tires remained consistent before and after installation of spiral fins on the outer wall of the inner cylinder. The maximum temperature difference of the material layer after pyrolysis, before and after installing spiral fins on the outer wall of the inner cylinder, was 11.2 °C. The results showed that the influence of spiral fins on the final temperature of the material layer was limited.

The apparent heat transfer coefficients between the materials and the inner surface of the pyrolysis furnace, before and after installing spiral fins, were calculated based on the measured material temperatures, as shown in Figure 16.



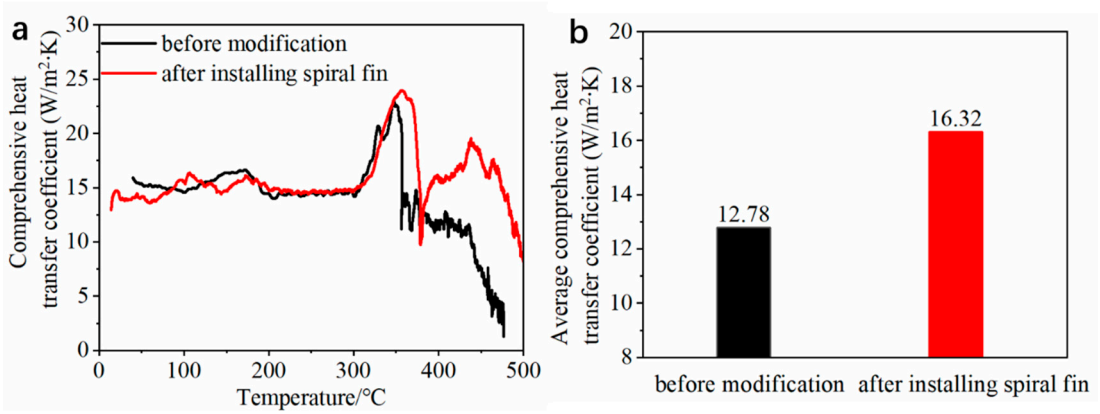
(a) Variation of apparent heat transfer coefficient with temperature

(b) Average apparent heat transfer coefficient

Figure 16. The apparent heat transfer coefficient between the inner wall of the inner.

After installing spiral fins on the outer wall of the inner cylinder of the rotary pyrolysis furnace, the maximum value of the apparent heat transfer coefficient in the water evaporation stage was higher than that before the modification. Subsequently, it decreased as the temperature increased, with a sharp decline observed at 370 °C. As shown in Figure 16b, the average apparent heat transfer coefficients before and after the modification were 179.94 W/(m^2·K) and 204.06 W/(m^2·K), with an increase of 13.60%, demonstrating that installation of spiral fins on the outer wall of the inner cylinder can significantly enhance heat transfer.

The comprehensive heat transfer coefficients before and after installation of spiral fins are shown in Figure 17.



(a) Variation of comprehensive heat transfer coefficient with temperature

(b) Average comprehensive heat transfer coefficient

Figure 17. Comprehensive heat transfer performance of the rotary pyrolysis furnace before and after modification.

4. Conclusions

In this study, the effects of tire particle size, rotary furnace rotation speed, addition of enhanced heat transfer materials, installation of spiral fins on the transfer performance, and distribution of pyrolysis products were investigated experimentally, and the following conclusions were drawn:

(1) During the process of waste tire pyrolysis, the use of powder particles ensured uniform heating, achieving the maximum comprehensive heat transfer coefficient of 12.78 W/(m^2·K) and the highest liquid products of 44.7%. However, the fine particles resulted in localized overheating, leading to deeper cracking and increased gaseous products.

(2) At a rotational speed of 3 rpm for the rotary pyrolysis furnace, there was sufficient contact between material and kiln wall, achieving the maximum comprehensive heat transfer coefficient 12.78 W/(m^2·K). The liquid product proportion was highest at rotational speeds of 1.5 rpm and 3 rpm, accounting for 45.0% and 44.7%, respectively.

(3) Adding carborundum or white alundum was beneficial for improving the heat transfer performance and heat transfer uniformity during the pyrolysis process, enhancing the pyrolysis efficiency, and reducing energy consumption, with comprehensive heat transfer coefficients of 13.53 W/(m^2·K) and 13.20 W/(m^2·K). Among them, there was a positive effect on the enhancement of the proportion of liquid product by adding carborundum, which increased to 46.1%.

(4) Compared with the unmodified pyrolysis chamber, the heat transfer enhancement effect was very obvious after the installation of spiral fins, and the comprehensive heat transfer coefficient was increased by 27.7% from 12.78 W/(m^2·K) to 16.32 W/(m^2·K).

(5) The operating parameters with the best heat transfer performance and the highest pyrolysis oil yield were obtained through this study, but these conclusions were obtained on small-scale experimental equipment and need to be verified through engineering practice before they can be promoted and applied.

Author Contributions: Writing—original draft preparation, H.M. and Y.B.; methodology, H.M.; validation, Y.B. and S.M.; writing—review and editing, S.M.; project administration, Y.B.; investigation, Z.Z. All authors have read and agreed to the published version of the manuscript.

Funding: This work is supported by the National Key Research and Development Program of China (No. 2022YFC3902300).

Data Availability Statement: The original contributions presented in this study are included in the article. Further inquiries can be directed to the corresponding author.

Conflicts of Interest: The authors declare no conflicts of interest.

References

1. Hrynyshyn, K.; Skorokhoda, V.; Chervinskyy, T. Study on the composition and properties of pyrolysis 598pyrocondensate of used tires. *Chem. Chem. Technol.* **2022**, *16*, 159–163. [CrossRef]
2. Pyshyev, S.; Lypko, Y.; Demchuk, Y.; Kukhar, O.; Korchak, B.; Pochapska, I.; Zhytnetskyi, I. Characteristics and applications of waste tire pyrolysis products: A review. *Chem. Chem. Technol.* **2024**, *18*, 244–257. [CrossRef]
3. Adhikari, B.; Maiti, S. Reclamation and recycling of waste rubber. *Prog. Polym. Sci.* **2000**, *25*, 909–948. [CrossRef]
4. Xia, Y.; Yang, Y.; Zhu, C.; Ouyang, S.; Wang, J.; Li, L. Kinetic and thermodynamic characteristics in scrap tyres pyrolysis process and components analysis of pyrolysis oil. *Low-Carbon Chem. Chem. Eng.* **2023**, *48*, 36–44.
5. Qin, L.; Wang, L. Reaction kinetic analysis of waste tire pyrolysis catalyzed by WUST10. *Environ. Prot. Chem. Ind.* **2021**, *41*, 452–457.
6. Chang, Q.; Jin, L.; Feng, Z.X.; Li, A.; Shen, K. Research on the Control and Management of Atmospheric Pollutants in Waste Tire Pyrolysis Projects. *Fluid Meas. Control.* **2024**, *5*, 52–55.
7. Gao, N.; Wang, F.; Quan, C.; Santamaria, L.; Lopez, G.; Williams, P.T. Tire pyrolysis char: Processes, properties, upgrading and applications. *Prog. Energy Combust. Sci.* **2022**, *93*, 101022. [CrossRef]
8. Yang, Q.; Yu, S.; Zhong, H.; Liu, T.; Yao, E.; Zhang, Y.; Zou, H.; Du, W. Gas products generation mechanism during co-pyrolysis of styrene-butadiene rubber and natural rubber. *J. Hazard. Mater.* **2021**, *401*, 123302. [CrossRef]
9. Han, J.; Li, W.; Liu, D.; Qin, L.; Chen, W.; Xing, F. Pyrolysis characteristic and mechanism of waste tyre: A thermogravimetry-mass spectrometry analysis. *J. Anal. Appl. Pyrolysis* **2018**, *129*, 1–5. [CrossRef]
10. Kan, T.; Strezov, V.; Evans, T. Fuel production from pyrolysis of natural and synthetic rubbers. *Fuel* **2017**, *191*, 403–410. [CrossRef]
11. Zhang, H.L.; Fan, X.X.; Liu, Y.F. Experimental study on pyrolysis of blocky tires in a fixed-bed reactor. *Renew. Energy Resour.* **2015**, *33*, 149–153.
12. Caponero, J.; Tenório, J.A.S.; Levendis, Y.A.; Carlson, J.B. Emissions of batch combustion of waste tire chips: The afterburner effect. *Energy Fuels* **2003**, *17*, 225–239. [CrossRef]
13. Ziadat, A.H.; Sood, E. An environmental impact assessment of the open burning of scrap tires. *J. Appl. Polym. Sci.* **2014**, *14*, 2695–2703. [CrossRef]
14. Labaki, M.; Jeguirim, M. Thermochemical conversion of waste tyres—A review. *Environ. Sci. Pollut. Res.* **2017**, *24*, 9962–9992. [CrossRef]
15. Yan, D. *Study on the Utilization of Pyrolytic Products from Pyrolysis of Used Tyre in a Pilot-Scale Rotary Kiln and the Mechanism and Kinetic Model of Rubber Pyrolysis*; University of Zhejiang: Hangzhou, China, 2006.
16. Kar, Y. Catalytic pyrolysis of car tire waste using expanded perlite. *Waste Manag.* **2011**, *31*, 1772–1782. [CrossRef]
17. Galvagno, S.; Casu, S.; Casabianca, T.; Cornacchia, G. Pyrolysis process for the treatment of scrap tyres: Preliminary experimental results. *Waste Manag.* **2002**, *22*, 917–923. [CrossRef]
18. Yin, Z.J.; Zhang, H.; Han, T. Simulation of particle flow on an elliptical vibrating screen using the discrete element method. *Powder Technol.* **2016**, *302*, 443–454. [CrossRef]
19. Zhu, H.P.; Yu, A.B. A theoretical analysis of the force models in discrete element method. *Powder Technol.* **2006**, *161*, 122–129. [CrossRef]
20. Zhao, Y.; Yang, S.L.; Zhang, L.Q.; Chew, J.W. Understanding the varying discharge rates of lognormal particle size distributions from a hopper using the Discrete Element Method. *Powder Technol.* **2019**, *342*, 356–370. [CrossRef]
21. Tchapda, A.H.; Pisupati, S.V. A review of thermal co-conversion of coal and biomass/waste. *Energies* **2014**, *7*, 1098–1148. [CrossRef]
22. Undri, A.; Rosi, L.; Frediani, M.; Frediani, P. Upgraded fuel from microwave assisted pyrolysis of waste tire. *Fuel* **2014**, *115*, 600–608. [CrossRef]
23. Beaumontt, O.; Schwob, Y. Influence of physical and chemical parameters on wood pyrolysis. *Ind. Eng. Chem. Res. Des. Dev.* **1984**, *23*, 637–641. [CrossRef]
24. Oyedun, A.; Lam, K.L.; Fittkau, M.; Hui, C.W. Optimisation of particle size in waste tyre pyrolysis. *Fuel* **2012**, *95*, 417–424. [CrossRef]
25. Kaminsky, W.; Mennerich, C.; Zhang, Z. Feedstock recycling of synthetic and natural rubber by pyrolysis in a fluidized bed. *J. Anal. Appl. Pyrolysis* **2009**, *85*, 334–337. [CrossRef]

26. Raj, R.E.; Kennedy, Z.R.; Pillai, B.C. Optimization of process parameters in flash pyrolysis of waste tyres to liquid and gaseous fuel in a fluidized bed reactor. *Energy Convers. Manag.* **2013**, *67*, 145–151. [CrossRef]
27. Cheng, Z.; Liang, J.; Kawamura, K.; Zhou, H.; Asamura, H.; Uratani, H.; Tiwari, J.; Graham, S.; Ohno, Y.; Nagai, Y.; et al. High thermal conductivity in wafer-scale cubic silicon carbide crystals. *Nat. Commun.* **2022**, *13*, 7201. [CrossRef]
28. Xia, J.; Qin, Y.; Wei, X.; Li, L.; Li, M.; Kong, X.; Xiong, S.; Cai, T.; Dai, W.; Lin, C.-T.; et al. Enhanced Thermal Conductivity of Polymer Composite by Adding Fishbone-like Silicon Carbide. *Nanomaterials* **2021**, *11*, 2891. [CrossRef]
29. AbdulKarim-Talaq, M.; Hassan, K.T.; Hameed, D.A. Improvement of thermal conductivity of novel asymmetric dimeric coumarin liquid crystal by doping with boron nitride and aluminium oxide nanoparticles. *Mater. Chem. Phys.* **2023**, *297*, 127367. [CrossRef]
30. Kedzierski, M.A.; Brignoli, R.; Quine, K.T.; Brown, J.S. Viscosity, density, and thermal conductivity of aluminum oxide and zinc oxide nanolubricants. *Int. J. Refrig.* **2017**, *74*, 3–11. [CrossRef]
31. Liu, L.; Cai, G.; Liu, X.; Liu, S.; Puppala, A.J. Evaluation of thermal-mechanical properties of quartz sand-bentonite-carbon fiber mixtures as the borehole backfilling material in ground source heat pump. *Energy Build.* **2019**, *202*, 109407. [CrossRef]
32. Ju, Z.; Lu, S.; Guo, K.; Liu, X. Changes in the thermal conductivity of soil with different salts. *J. Soils Sediments* **2023**, *23*, 3376–3383. [CrossRef]

Disclaimer/Publisher's Note: The statements, opinions and data contained in all publications are solely those of the individual author(s) and contributor(s) and not of MDPI and/or the editor(s). MDPI and/or the editor(s) disclaim responsibility for any injury to people or property resulting from any ideas, methods, instructions or products referred to in the content.